Data in Brief 32 (2020) 106246

Contents lists available at ScienceDirect

Data in Brief

journal homepage: www.elsevier.com/locate/dib

Data Article

MRI data confirm the selective involvement of thalamic and amygdalar nuclei in amyotrophic lateral sclerosis and primary lateral sclerosis ☆

Rangariroyashe H. Chipika [a], We Fong Siah [a], Stacey Li Hi Shing [a], Eoin Finegan [a], Mary Clare McKenna [a], Foteini Christidi [b], Kai Ming Chang [a,c], Efstratios Karavasilis [d], Alice Vajda [e], Jennifer C. Hengeveld [e], Mark A. Doherty [e], Colette Donaghy [f], Siobhan Hutchinson [g], Russell L. McLaughlin [e], Orla Hardiman [a], Peter Bede [a,*]

[a] *Computational Neuroimaging Group, Biomedical Sciences Institute, Trinity College Dublin, Ireland*
[b] *First Department of Neurology, Aeginition Hospital, National and Kapodistrian University of Athens, Greece*
[c] *Electronics and Computer Science, University of Southampton, United Kingdom*
[d] *2nd Department of Radiology, Attikon University Hospital, University of Athens, Athens, Greece*
[e] *Complex Trait Genomics Laboratory, Smurfit Institute of Genetics, Trinity College Dublin, Ireland*
[f] *Department of Neurology, Western Health & Social Care Trust, Belfast, Northern Ireland, United Kingdom*
[g] *Department of Neurology, St James's Hospital Dublin, Ireland*

ARTICLE INFO

Article history:
Received 4 August 2020
Revised 12 August 2020
Accepted 25 August 2020
Available online 1 September 2020

Keywords:
Motor neuron disease
Amyotrophic lateral sclerosis
Primary lateral sclerosis
Thalamus
Neuroimaging

ABSTRACT

A standardised imaging protocol was implemented to evaluate disease burden in specific thalamic and amygdalar nuclei in 133 carefully phenotyped and genotyped motor neuron disease patients. "Switchboard malfunction in motor neuron diseases: selective pathology of thalamic nuclei in amyotrophic lateral sclerosis and primary lateral sclerosis" [1] "Amygdala pathology in amyotrophic lateral sclerosis and primary lateral sclerosis" [2] Raw volumetric data, group comparisons, effect sizes and percentage change are presented. Both ALS and PLS patients exhibited focal thalamus atrophy in ventral lateral and ventral anterior regions revealing extrapyramidal motor degeneration. Reduced acces-

☆ **Category / Subject area**: Neuroscience (Neurology)
DOI of original article: 10.1016/j.nicl.2020.102300
* Corresponding author.
E-mail address: bedep@tcd.ie (P. Bede).

https://doi.org/10.1016/j.dib.2020.106246

sory basal nucleus and cortical nucleus volumes were noted in the amygdala of *C9orf72* negative ALS patients compared to healthy controls. ALS patients carrying the GGGGCC hexanucleotide repeats in *C9orf72* exhibited preferential pathology in the mediodorsal-paratenial-reuniens thalamic nuclei and in the lateral nucleus and cortico-amygdaloid transition area of the amygdala. Considerable thalamic atrophy was observed in the sensory nuclei and lateral geniculate region of PLS patients. Our data demonstrate genotype-specific patterns of thalamus and amygdala involvement in ALS and a distinct disease-burden pattern in PLS. The dataset may be utilised for validation purposes, meta-analyses and the interpretation of thalamic and amygdalar profiles from other ALS genotypes.

Specifications Table

Subject	Neurology, Amyotrophic Lateral Sclerosis, Primary Lateral Sclerosis, Radiology, Neuroimaging
Specific subject area	MRI, Grey matter volumetry, Thalamus
Type of data	Magnetic resonance imaging: quantitative neuroimaging metrics data form a standardised acquisition protocol
How data were acquired	Imaging data were acquired on a Philips Achieva 3T MRI scanner (Philips Medical Systems, Best, The Netherlands) with an 8-channel head coil.
Data format	The volumetric profile of thalamic nuclei are presented as raw data, percentage change, and comparative p-values corrected for age, gender, education and total intracranial volumes
Parameters for data collection	3D T1-weighted sequence: spatial resolution: $1 \times 1 \times 1$ mm, Field of view: $256 \times 256 \times 160$ mm, repetition time=8.5 ms, Echo time = /3.9 ms, Inversion time =1060 ms, flip angle = 8°, SENSE factor = 1.5, sagittal acquisition; 256 slices.
Description of data collection	Data were collected on a 3 Tesla MRI system. Demographic variables were recorded before the MRI scan, and a standardised neurological examination was also performed on the day of the MRI.
Data source location	Institution: Computational neuroimaging group, Trinity Biomedical Sciences Institute, Trinity College Dublin City/Town/Region: Dublin Country: Ireland
Data accessibility	Raw volumetric data are available online at Mendeley Data; http://dx.doi.org/10.17632/hchj4w6zck.2
Related research article	Authors: Rangariroyashe H. Chipika, Eoin Finegan, Stacey Li Hi Shing, Mary Clare McKenna, Kai Ming Chang, Mark A. Doherty, Jennifer C. Hengeveld, Alice Vajda, Niall Pender, Siobhan Hutchinson, Colette Donaghy, Russell L. McLaughlin, Orla Hardiman, Peter Bede Title: "Switchboard" malfunction in motor neuron diseases: Selective pathology of thalamic nuclei in amyotrophic lateral sclerosis and primary lateral sclerosis Journal: Neuroimage Clinical DOI: Neuroimage Clin. 2020 May 30;27:102300. doi: 10.1016/j.nicl.2020.102300. Authors: Rangariroyashe H. Chipika, Foteini Christidi, Eoin Finegan, Stacey Li Hi Shing, Mary C. McKenna, Kai Ming Chang, Mark A. Doherty, Jennifer C. Hengeveld, Alice Vajda, Niall Pender, Siobhan Hutchinson, Colette Donaghy, Russell L. McLaughlin, Orla Hardiman, Peter Bede Title: Amygdala pathology in amyotrophic lateral sclerosis and primary lateral sclerosis Journal: Journal of the neurological sciences DOI: 10.1016/j.jns.2020.117039.

Value of the Data

- The volumetric profile of thalamic and amygdalar nuclei in *C9orf72* allows the comparative assessment of imaging findings in other ALS genotypes.
- The presented dataset may aid the interpretation of MRI data from asymptomatic *C9orf72* hexanucleotide carriers.
- The data also permit meta-analyses across multiple data sources.
- Reference thalamic and amygdala data form healthy controls may be utilised for the interpretation of imaging findings in other neurological conditions.

1. Data Description

In this dataset we present the volumetric profile of thalamic nuclei in 12 ALS patients carrying the GGGGCC hexanucleotide repeat expansion in C9orf72, 88 *C9orf72* negative ALS patients, 33 PLS patients and 117 age and gender-matched healthy controls. The demographic, genetic and clinical characteristics of study participants are reported in the companion articles [1,2]. Table 1. Raw volumetric data are available online at Mendeley Data; http://dx.doi.org/10.17632/hchj4w6zck.2. and http://dx.doi.org/10.17632/28mhksbnsy.2. Raw volumetric profiles in each study group and statistically significant intergroup differences are also presented in Fig. 1 and Fig. 2. Effect sizes for volumetric differences between the study groups are presented in Table 2. Percentage change in thalamic and amygdalar nuclei with respect of healthy controls is shown in Fig. 3., ranking the most affected regions in each patient cohort.

2. Experimental Design, Materials, and Methods

The neuroimaging signature of ALS is associated with motor cortex [3], corticospinal tract [4], corpus callosum [5,6], brainstem [7], and spinal cord pathology [8]. Neuropsychological manifestations [9,10] and extra-motor pathology [11,12] have also been gradually characterised [11,12]. Thalamus pathology is increasingly recognised in ALS [13-16], but limited information is available in PLS [14,17]. This neuroimaging study was approved by the relevant institutional ethic committee and all participants provided informed consent. Thirty-three patients with primary lateral sclerosis, 100 patients with amyotrophic lateral sclerosis and 117 healthy controls were included in this study. Patients with ALS were stratified for the presence of GGGGCC hexanucleotide expansion in *C9orf72*. All patients underwent standardised clinical assessment. [10] The study was specifically designed to characterise thalamus degeneration in ALS and PLS and identify distinguishing imaging characteristics between the two conditions. [17,18] Total intracranial volumes (TIV) were estimated using FSL-FIRST of the FMRIB's Software Library (FSL). The thalamus was segmented into 25 sub-regions using a Bayesian parcellation algorithm based on a probabilistic atlas [19].

The thalamic and amygdalar profiles of study groups were evaluated with respect to each nucleus. Statistically significant intergroup differences were identified following corrections for age, gender, education, TIV and multiple comparisons [20]. Fig. 1**.** In addition, Cohen's |d| was calculated to interpret intergroup differences in nuclear volumes. $|d| \geq 0.80$ was considered a large effect size; 0.50–0.79 a medium effect size; and 0.20–0.49 regarded as a small effect size. Table 2. To evaluate which nuclei were most affected in the patient groups and rank their involvement, percentage change was calculated in each nucleus with reference to the estimated marginal means of healthy controls. Based on this analysis, the most significantly affected thalamic nuclei in the ALS C9+ cohort are the laterodorsal nuclei, followed by mediodorsal-paratenial-reuniens and anteroventral regions. In the ALS C9- cohort, the laterodorsal nuclei were also the most atrophic structure, followed by the anteroventral region. In the PLS cohort, the most significant volume reductions were observed in sensory nuclei and the lateral geniculate. Fig. 3. In

Table 1
Data categories and measures ALS = amyotrophic lateral sclerosis; ALSFRS-*r* = amyotrophic lateral sclerosis functional rating scale-revised; PLS = Primary lateral sclerosis; C9+ = *C9orf72* hexanucleotide carrier, C9- = *C9orf72* non-carrier, HC – Healthy Control, Rt-Right, Lt-Left.

Data categories	Specific Measures
Demographic variables	Age (years)
	Gender (Male/Female)
	Years of education (years)
	Handedness (Rt/Lt)
	Site of onset (Limb/Bulbar)
	Diagnosis (C9+ALS, C9-ALS, PLS, HC)
Thalamic nucleus volumes	Anteroventral (mm^3)
	Lateral geniculate (mm^3)
	Medial geniculate (mm^3)
	Pulvinar/Limitans (mm^3)
	Laterodorsal (mm^3)
	Lateroposterior (mm^3)
	Mediodorsal/Paratenial/Reuniens (mm^3)
	Motor Hub (mm^3)
	Sensory Hub (mm^3)
	Intralaminar (mm^3)
Amygdaloid nuclei volumes	Lateral nucleus (mm^3)
	Basal nucleus (mm^3)
	Accessory basal nucleus (mm^3)
	Anterior amygdaloid area (mm^3)
	Central nucleus (mm^3)
	Medial nucleus (mm^3)
	Cortical nucleus (mm^3)
	Corticoamygdaloid transition (mm^3)
	Paralaminar nucleus (mm^3)
	Whole amygdala (mm^3)
Effect sizes of intergroup differences Cohen's |d|	C9+ALS versus healthy controls
	C9-ALS versus healthy controls
	PLS versus healthy controls
	C9+ALS versus C9-ALS
	C9+ALS versus PLS
	C9-ALS versus PLS
Percentage change with respect to estimated marginal means of healthy controls	Anteroventral (mm^3)
	Lateral geniculate (mm^3)
	Medial geniculate (mm^3)
	Pulvinar/Limitans (mm^3)
	Laterodorsal (mm^3)
	Lateroposterior (mm^3)
	Mediodorsal/Paratenial/Reuniens (mm^3)
	Motor Hub (mm^3)
	Sensory Hub (mm^3)
	Intralaminar (mm^3)
	Lateral nucleus (mm3)
	Basal nucleus (mm3)
	Accessory basal nucleus (mm3)
	Anterior amygdaloid area (mm3)
	Central nucleus (mm3)
	Medial nucleus (mm3)
	Cortical nucleus (mm3)
	Corticoamygdaloid transition (mm3)
	Paralaminar nucleus (mm3)
	Whole amygdala (mm3)

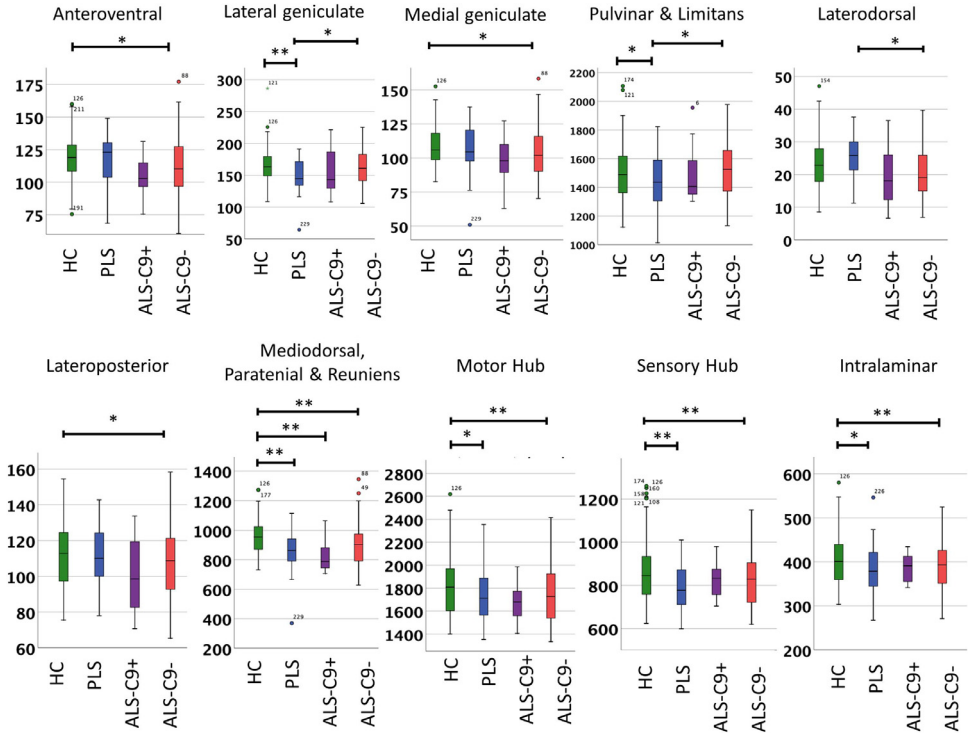

Fig. 1. The volumetric profile of thalamic nuclei in *C9orf72* hexanucleotide carrying ALS patients (ALS C9+), *C9orf72* negative amyotrophic lateral sclerosis patients (ALS C9-), primary lateral sclerosis patients (PLS) and healthy controls (HC). Statistically significant intergroup differences following correction for age, gender, intracranial volumes and multiple comparisons are indicated with asterisks. * $p < 0.05$ ** $p < 0.01$.

the amygdala, the most significantly affected structures in the ALS C9+ cohort are the cortico-amygdaloid transition area, followed by accessory-basal nucleus and the lateral nucleus. In the ALS C9- cohort, the cortical nucleus was also the most atrophic structure, followed by the medial nucleus and the anterior amygdaloid nucleus. We found no evidence of amygdala atrophy in the PLS cohort, either by the assessment of the entire structure or the analysis of the specific nuclei.

Declaration of Competing Interest

None declared.

Acknowledgements

We thank all the patients with ALS and PLS for participating in this research study and we are also grateful for the participation of the healthy controls. This study was supported by the Spastic Paraplegia Foundation, Inc. (SPF). Professor Peter Bede is also supported by the Health Research Board (HRB EIA-2017–019), the EU Joint Programme – Neurodegenerative Disease Research (JPND), the Andrew Lydon scholarship, the Irish Institute of Clinical Neuroscience (IICN), and the Iris O'Brien Foundation; he is the patron of the Irish Motor Neuron Disease Associa-

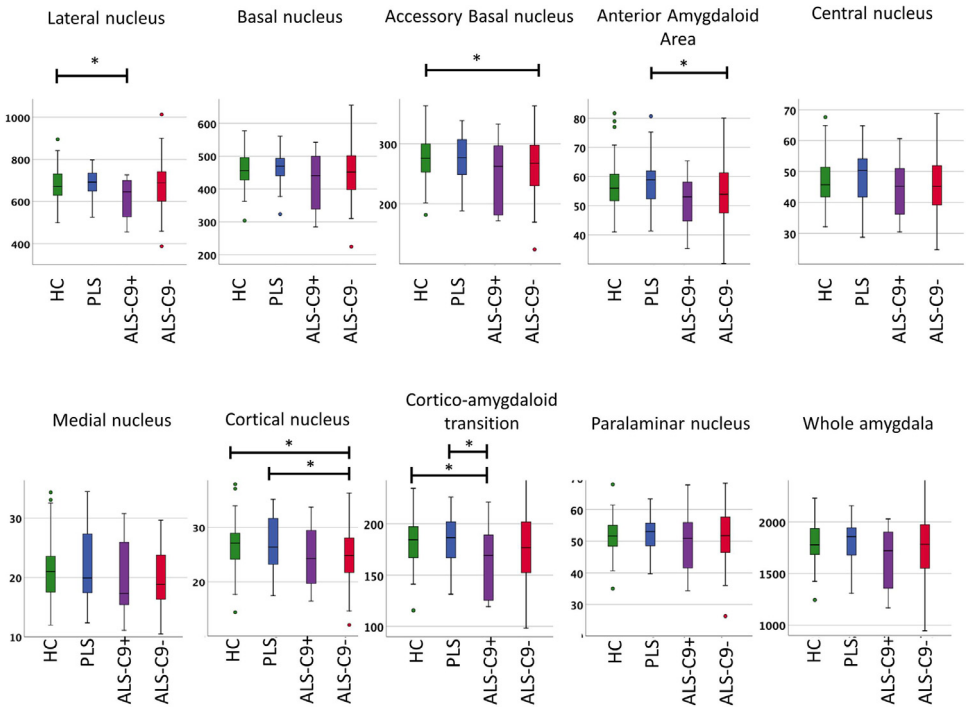

Fig. 2. The raw volumetric profile of amygdalar nuclei in *C9orf72* hexanucleotide carrying ALS patients (ALS-C9+), *C9orf72* negative amyotrophic lateral sclerosis patients (ALS-C9-), primary lateral sclerosis patients (PLS) and healthy controls (HC). Statistically significant intergroup differences following corrections for age, gender, intracranial volumes and multiple comparisons are indicated with asterisks. * $p < 0.05$.

tion (IMNDA). Doctor Foteini Christidi is supported by the EU-IKY Scholarship Program (European Social Fund-ESF), the Greek "Reinforcement of Postdoctoral Researchers" grant (5033021) of the "Human Resources Development Program, Education and Lifelong Learning" of the National Strategic Reference Framework (NSRF 2014–2020). Professor Russell L McLaughlin is supported by the Motor Neurone Disease Association (957–799) and Science Foundation Ireland (17/CDA/4737). Mr. Mark A Doherty is supported by Science Foundation Ireland (15/SPP/3244). The sponsors had no role in the design of the study, data analyses, or the decision to submit these findings for publication.

Table 2
Effect sizes for intergroup differences using Cohen's |d|. A '|d|' value over 0.80 is considered a large effect size and is shown in red; 0.50–0.79 signifies a medium effect size and is highlighted in green, 0.20–0.49 is regarded as a small effect size and is shown in yellow, |d| < 0.19 is a negligible effect size and is presented in grey.

Thalamic nuclei	C9+ALS versus HC	C9-ALS versus HC	PLS versus HC	C9+ALS versus C9-ALS	C9+ALS versus PLS	C9-ALS versus PLS
Anteroventral	0.7	0.44	0.27	0.26	0.44	0.18
Lateral geniculate	0.48	0.17	0.79	0.31	0.32	0.62
Medial geniculate	0.66	0.37	0.19	0.3	0.48	0.18
Pulvinar-limitans	0.01	0.07	0.61	0.06	0.61	0.54
Laterodorsal	0.5	0.32	0.28	0.17	0.79	0.6
Lateroposterior	0.58	0.37	0.1	0.21	0.49	0.27
Mediodorsal-paratenial-reuniens	1.27	0.59	0.94	0.68	0.34	0.34
Motor hub	0.56	0.48	0.59	0.08	0.03	0.11
Sensory hub	0.27	0.56	0.88	0.29	0.63	0.32
Intralaminar	0.2	0.49	0.58	0.29	0.39	0.09
Whole Thalamus	0.64	0.53	0.86	0.11	0.23	0.34
Whole amygdala	-0.8	-0.32	-0	-0.47	-0.77	-0.3
Lateral nucleus	-0.8	-0.24	-0.1	-0.59	-0.73	-0.14
Basal nucleus	-0.7	-0.28	0	-0.45	-0.72	-0.28
Accessory basal nucleus	-0.8	-0.42	-0	-0.39	-0.77	-0.39
Anterior amygdaloid area	-0.6	-0.29	0.29	-0.29	-0.86	-0.57
Central nucleus	-0.29	-0.29	0.00	0.00	-0.29	-0.29
Medial nucleus	-0.25	-0.50	0.25	0.25	-0.50	-0.75
Cortical nucleus	-0.67	-0.33	0.33	-0.33	-1.00	-0.67
Cortico-amygdaloid transition	-0.90	-0.35	0.00	-0.55	-0.90	-0.35
Paralaminar nuclues	-0.40	-0.20	0.00	-0.20	-0.40	-0.20

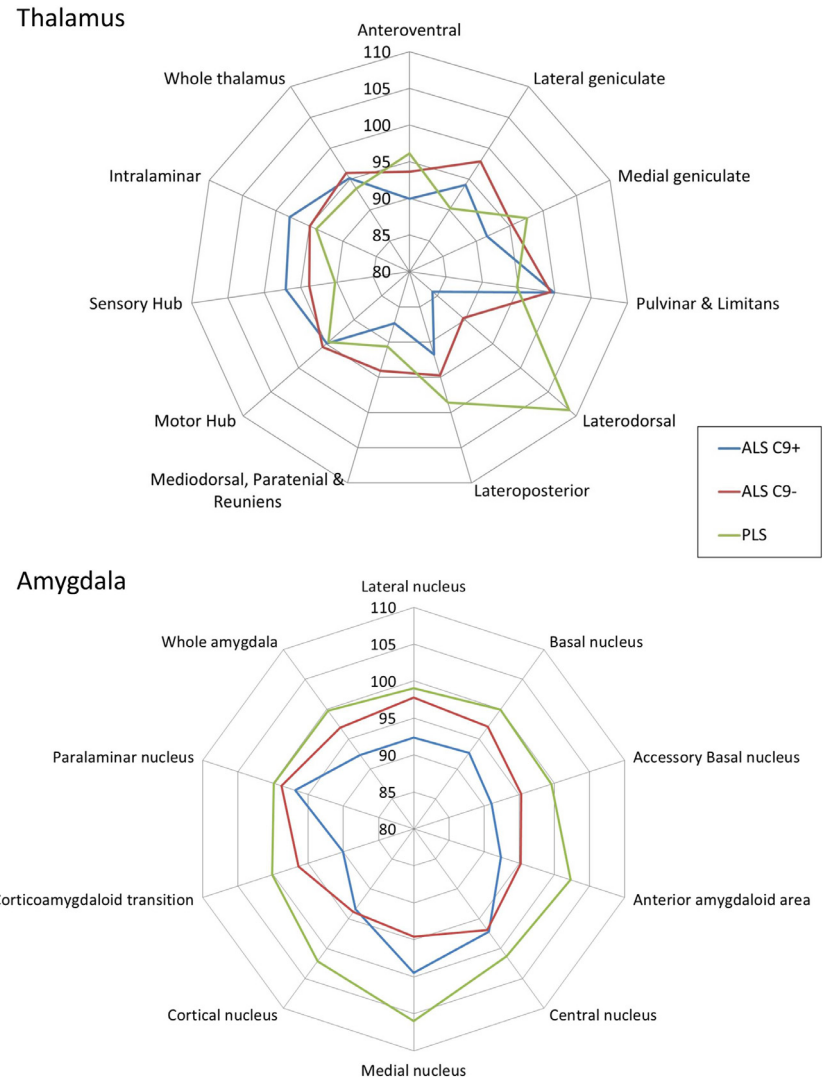

Fig. 3. The segmental thalamus and amygdala profile of C9+ ALS, C9- ALS, and PLS with reference to healthy controls. 100% represents the estimated marginal mean of healthy controls for each structure. Estimated marginal means of volumes were calculated with the following values age = 59.07, gender = 1.43, Education = 13.68, total intracranial volume = 1,432,347.15.

References

[1] R.H. Chipika, et al., "Switchboard" malfunction in motor neuron diseases: selective pathology of thalamic nuclei in amyotrophic lateral sclerosis and primary lateral sclerosis, Neuroimage Clin. 27 (2020) 102300.

[2] R.H. Chipika, et al., Amygdala pathology in amyotrophic lateral sclerosis and primary lateral sclerosis, J. Neurol. Sci. (2020) 117039.

[3] C. Schuster, O. Hardiman, P. Bede, Development of an automated MRI-based diagnostic protocol for amyotrophic lateral sclerosis using disease-specific pathognomonic features: a quantitative disease-state classification study, PLoS One 11 (12) (2016) e0167331.

[4] P. Bede, et al., *Virtual brain biopsies in amyotrophic lateral sclerosis: diagnostic classification based on* in vivo *pathological patterns*, Neuroimage Clin. 15 (2017) 653–658.

[5] B. Nasseroleslami, et al., Characteristic increases in EEG connectivity correlate with changes of structural MRI in amyotrophic lateral sclerosis, Cereb. Cortex 29 (1) (2019) 27–41.

[6] C. Schuster, et al., The segmental diffusivity profile of amyotrophic lateral sclerosis associated white matter degeneration, Eur. J. Neurol. 23 (8) (2016) 1361–1371.

[7] P. Bede, et al., Brainstem pathology in amyotrophic lateral sclerosis and primary lateral sclerosis: a longitudinal neuroimaging study, Neuroimage Clin. 24 (2019) 102054.

[8] G. Querin, et al., Multimodal spinal cord MRI offers accurate diagnostic classification in ALS, J. Neurol. Neurosurg. Psychiatry 89 (11) (2018) 1220–1221.

[9] T. Burke, et al., *A Cross-sectional population-based investigation into behavioral change in amyotrophic lateral sclerosis: subphenotypes, staging, cognitive predictors, and survival*., Ann. Clin. Transl. Neurol. 4 (5) (2017) 305–317.

[10] M. Elamin, et al., Identifying behavioural changes in ALS: validation of the Beaumont Behavioural Inventory (BBI), Amyotroph Lateral Scler Frontotemporal Degener 18 (1–2) (2017) 68–73.

[11] F. Christidi, et al., Clinical and radiological markers of extra-motor deficits in amyotrophic lateral sclerosis, Front. Neurol. 9 (2018) 1005.

[12] T. Omer, et al., Neuroimaging patterns along the ALS-FTD spectrum: a multiparametric imaging study, Amyotroph Lateral Scler Frontotemporal Degener 18 (7–8) (2017) 611–623.

[13] P. Bede, et al., *The selective anatomical vulnerability of ALS: 'disease-defining' and 'disease-defying' brain regions*., Amyotroph Lateral Scler Frontotemporal Degener 17 (7–8) (2016) 561–570.

[14] E. Finegan, et al., Widespread subcortical grey matter degeneration in primary lateral sclerosis: a multimodal imaging study with genetic profiling, Neuroimage Clin. 24 (2019) 102089.

[15] P. Bede, et al., Connectivity-based characterisation of subcortical grey matter pathology in frontotemporal dementia and ALS: a multimodal neuroimaging study, Brain Imaging Behav. 12 (6) (2018) 1696–1707.

[16] P. Bede, G. Querin, P.F. Pradat, The changing landscape of motor neuron disease imaging: the transition from descriptive studies to precision clinical tools, Curr. Opin. Neurol. 31 (4) (2018) 431–438.

[17] E. Finegan, et al., Primary lateral sclerosis: a distinct entity or part of the ALS spectrum? Amyotroph Lateral Scler Frontotemporal Degener 20 (3–4) (2019) 133–145.

[18] E. Finegan, et al., The clinical and radiological profile of primary lateral sclerosis: a population-based study, J. Neurol. 266 (11) (2019) 2718–2733..

[19] J.E. Iglesias, et al., *A probabilistic atlas of the human thalamic nuclei combining ex vivo MRI and histology*., Neuroimage 183 (2018) 314–326.

[20] P. Bede, et al., Sexual dimorphism in ALS: exploring gender-specific neuroimaging signatures, Amyotroph Lateral Scler Frontotemporal Degener 15 (3–4) (2014) 235–243.